brain sciences

MDPI

Article

Temporal Stability of Dynamic Default Mode Network Connectivity Negatively Correlates with Suicidality in Major Depressive Disorder

Xuan Ouyang [1,†], Yicheng Long [1,†], Zhipeng Wu [1], Dayi Liu [1], Zhening Liu [1] and Xiaojun Huang [2,*]

[1] Department of Psychiatry, National Clinical Research Center for Mental Disorders, The Second Xiangya Hospital, Central South University, Changsha 410011, China
[2] Department of Psychiatry, Jiangxi Provincial People's Hospital, The First Affiliated Hospital of Nanchang Medical College, Nanchang 330006, China
* Correspondence: xiaojunh9@163.com
† These authors contributed equally to this work.

Abstract: Previous studies have demonstrated that the suicidality in patients with major depressive disorder (MDD) is related to abnormal brain functional connectivity (FC) patterns. However, little is known about its relationship with dynamic functional connectivity (dFC) based on the assumption that brain FCs fluctuate over time. Temporal stabilities of dFCs within the whole brain and nine key networks were compared between 52 MDD patients and 21 age, sex-matched healthy controls (HCs) using resting-state functional magnetic resonance imaging and temporal correlation coefficients. The alterations in MDD were further correlated with the scores of suicidality item in the Hamilton Rating Scale for Depression (HAMD). Compared with HCs, the MDD patients showed a decreased temporal stability of dFC as indicated by a significantly decreased temporal correlation coefficient at the global level, as well as within the default mode network (DMN) and subcortical network. In addition, temporal correlation coefficients of the DMN were found to be significantly negatively correlated with the HAMD suicidality item scores in MDD patients. These results suggest that MDD may be characterized by excessive temporal fluctuations of dFCs within the DMN and subcortical network, and that decreased stability of DMN connectivity may be particularly associated with the suicidality in MDD.

Keywords: major depressive disorder; suicide; neuroimaging; fMRI; dynamic functional connectivity; dynamic brain network

Citation: Ouyang, X.; Long, Y.; Wu, Z.; Liu, D.; Liu, Z.; Huang, X. Temporal Stability of Dynamic Default Mode Network Connectivity Negatively Correlates with Suicidality in Major Depressive Disorder. *Brain Sci.* **2022**, *12*, 1263. https://doi.org/10.3390/brainsci12091263

Academic Editors: Ancha Baranova, Fuquan Zhang, Hongbao Cao and Andrew Clarkson

Received: 22 August 2022
Accepted: 15 September 2022
Published: 17 September 2022

1. Introduction

Major depressive disorder (MDD) is one of the leading causes of disability worldwide, partly because of the high rates of suicide attempts in MDD patients [1,2]. Neuroimaging studies using the resting-state functional magnetic resonance imaging (fMRI) have documented that the changes in functional connectivity (FC) between specific brain regions, such as increased precuneus-motor connectivity [3], increased amygdala-precuneus connectivity [4] and decreased fronto-limbic connectivity [5], are associated with increased suicidality in MDD. These suicidality-related alterations in brain functions may have important implications for understanding and preventing suicide among MDD patients.

The conventional fMRI studies assume that the patterns of brain FC are stationary. Recently, the brain FC was found to fluctuate over time even during rest, implying that describing it in a "static" manner might be too simplistic [6,7]. Therefore, the "dynamic functional connectivity (dFC)" has become a new topic in recent years to capture the fluctuations of brain connectivity [8–10]. With regard to MDD, some previous studies have provided initial evidence that MDD is associated with a decreased temporal stability (increased temporal variability) of dFC within multiple brain regions such as the medial

prefrontal cortex [11,12] and posterior cingulate cortex [13] within the default mode network (DMN), as well as the pallidum [14]. As for studies on the relationships between dFC and suicidality in MDD, several recent studies have found that the overall topological properties of dynamic connectomic [15], the dynamic degree centrality [16], and the dynamic amplitude of low-frequency fluctuation [17] could differentiate the MDD patients with and without suicidal ideation, implying the possible association between the abnormal fluctuations of brain dFC and suicidality in MDD. In a recent study, it was further found that compared with MDD patients without suicidal ideation, those patients with suicidal ideation showed increased dFC variability from the habenula to the superior temporal gyrus and precuneus [18]. Despite the accumulating findings, however, most of the above-mentioned studies are limited by that they only focused on dFC at the level of voxels or within specific regions of interests (ROIs). Recent studies have proved that abnormal dFC patterns in psychiatric disorders are not constrained in a circumscribed area but usually associated with the entire large-scale brain systems [19,20]. Nevertheless, how the changes in dFC within specific large-scale brain networks would be related to the suicidal ideation or behavior in MDD remains largely unknown to our knowledge.

In this study, we aimed to explore the possible relationships between temporal stabilities of large-scale brain dFCs and suicidality in MDD using the dynamic network model and a validated metric, the temporal correlation coefficient [12,21–23]. We firstly investigated the alterations in temporal correlation coefficients in MDD patients at the levels of whole brain and nine well-established key networks including the sensorimotor, visual, auditory, default-mode, frontoparietal, cingulo-opercular, salience, subcortical, and attention networks [24,25], respectively. After that, we further investigated their relationships with the level of suicidality in MDD patients. We hypothesized that (1) the previously reported findings in MDD, such as a decreased temporal stability of dFC within the DMN [11,12], would be replicated in the present sample; (2) the temporal stability of dFC within at least one network would be related with the level of suicidality in MDD.

2. Materials and Methods

2.1. Participants and Measures of Suicidality

The analyzed sample consisted of a total of 52 patients with MDD and 21 age-, sex-matched healthy controls (HCs), who were recruited from the Second Xiangya Hospital of Central South University, Changsha, China. All participants included were right-handed, Han Chinese adults with at least 6 years of education. All patients met the Diagnostic and Statistical Manual of Mental Disorders-IV (DSM-IV) criteria for MDD and had a 17-item Hamilton Rating Scale for Depression (HAMD) score > 7. All participants had no history of any substance abuse, any other neurological disorder, any contraindication to fMRI scanning or any history of electroconvulsive therapy. The HCs additionally met the following inclusion criteria: had no personal or family (in first-degree relatives) history of any mental illness as evaluated by the Structured Clinical Interview for DSM-IV (SCID). Note that the initial sample consisted of 58 MDD patients and 22 HCs; 6 patients and 1 healthy subject were excluded because of excessive head motion (see later in Section 2.2). The study was approved by the Ethics Committee of the Second Xiangya Hospital of Central South University, and written informed consent was obtained from all participants.

For all MDD patients, the level of current suicidality was assessed using the score of the HAMD item 3 (suicidality item), which ranges from 0 to 4. Using a single suicide item from depression scales to assess suicidality in psychiatric disorders has been proved to be valid [26–28].

2.2. Data Acquisition and Preprocessing

Resting-state fMRI and T1-weighted structural images were acquired on a 3.0 T MRI scanner (Philips Achieva XT). The fMRI images were obtained by gradient echo-planar imaging sequence (repetition time/echo time = 2000/30 ms; slice number = 36; thickness/gap = 4.0/0 mm; field of view = 240 × 240 mm^2; acquisition matrix = 64 × 64; flip angle = 90°; number of time points = 250),

and the T1-weighted images were obtained by three-dimensional fast spoiled gradient recalled sequence (repetition time/echo time = 7.5/3.7 ms; slice number = 180; thickness/gap = 1.0/0 mm; field of view = 240 × 240 mm^2; acquisition matrix 256 × 200; flip angle = 8°).

Data preprocessing was performed using the standard pipeline provided by the DPARSF software [29,30]. Briefly, it included removing the first 10 volumes, slice-timing, head motion realignment, brain tissue segmentation, spatial normalization, temporal filtering (0.01–0.10 Hz), and regressing out the signals from white matter, cerebrospinal fluid, and whole brain as well as the Friston-24 head motion parameters [31,32]. All images have been manually checked by trained researchers to ensure good quality. Moreover, 6 patients and 1 healthy subject with excessive head motion were excluded from the analysis, as determined by a mean framewise-displacement (FD) [33] > 0.2 mm.

2.3. Dynamic Brain Network Model

The fluctuation of brain dFC patterns was estimated based on the commonly used multilayer dynamic network model [8–10]. The nodes in brain network were defined by the Automated Anatomical Labeling (AAL) atlas [34], which was validated in previous fMRI studies [35–37]. The names of each of the 90 nodes were listed in the Appendix A (Table A1).

The dynamic networks were constructed as summarized in Figure 1. First, the mean time series were extracted from each node by averaging the signals of all voxels within that node. The widely used sliding-window approach was then applied with a window length of 100 s and an incremental step of 6 s as recommended [12,38,39], dividing the time series into 64 time windows. Within each window, the whole-brain connectivity matrices were calculated using pairwise Pearson correlations. The connectivity matrices were then thresholded with a wide range of densities ranging from 0.01 to 0.50 with an increment interval of 0.01 [40]. For each density, only the connections that survived the given threshold were reserved and assigned a value of 1, and those that did not survive were assigned a value of 0. As a result, a dynamic network $G = (G_t)_{t = 1, 2, 3, \ldots, 64}$, where G_t is the binary subgraph representing brain dFC within the tth time window, was acquired at each density for each subject. The temporal correlation coefficient was then computed at each density separately.

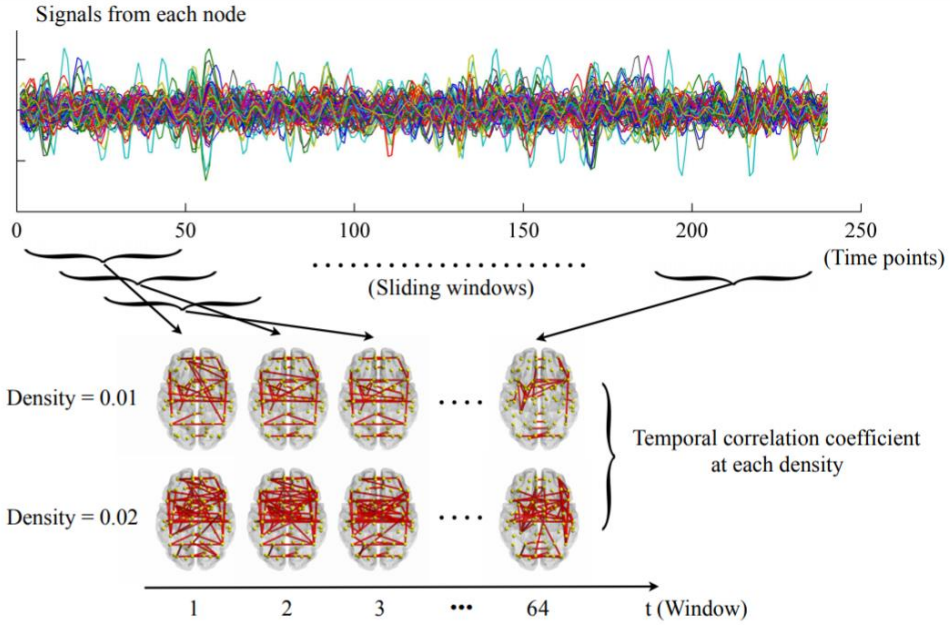

Figure 1. The steps for constructing dynamic networks and calculating temporal correlation coefficients as detailed in the Materials and Methods section (only the densities of 0.01 and 0.02 were presented here for visualization purposes).

2.4. Temporal Correlation Coefficient

Temporal correlation coefficient measures the stability of a dynamic network by the average overlap of all the connections between any two successive time windows as follows: firstly, let a_{ij} (t) = 1 if node i and node j are connected within the tth time window, and a_{ij} (t) = 0 if they are not. The nodal temporal correlation coefficient of the node i (C_i) is then defined as

$$C_i = \frac{1}{T-1} \sum_{t=1}^{T-1} \frac{\sum_j a_{ij}(t) a_{ij}(t+1)}{\sqrt{\left[\sum_j a_{ij}(t)\right]\left[\sum_j a_{ij}(t+1)\right]}} \quad (1)$$

where T is the number of time windows and N is the number of nodes in the network [12,21,22,41]. The C_i ranges from 0 to 1, and a higher value indicates a higher stability (lower variability) of node i. The C_i was computed and averaged across all densities (0.01 to 0.50) to ensure that the results would not be biased by a single threshold [12]. The temporal correlation coefficient of the whole brain is computed by averaging the C_i of all 90 nodes. To further investigate which brain systems were particularly affected, we assigned all nodes to the nine key networks as defined in previous studies [24,25,42] (see details in the Appendix A). The temporal correlation coefficient of each network was computed by averaging the C_i across all nodes of that network [22]. All computations were performed using two publicly available MATLAB toolboxes (https://sites.google.com/site/bctnet and https://github.com/asizemore/Dynamic-Graph-Metrics, accessed on 1 June 2022) [21,43]. The results were partly visualized using the BrainNet Viewer software [44].

2.5. Statistics

The demographic characteristics and mean FD were compared between the groups using the two-sample t-test or Chi-square test. Temporal correlation coefficients of the whole brain and each of the nine networks were compared between the groups of MDD patients and HCs using analysis of covariance (ANCOVA) covarying for age, sex, and education. The temporal correlation coefficient of whole brain or any network which showed significant between-group differences were further correlated with the total scores of HAMD and the scores of HAMD item 3 using Spearman's rank correlation coefficient, respectively. For multiple network-level comparisons and multiple correlation tests, the results were corrected by false discovery rate (FDR) and considered significant when the corrected $p < 0.05$.

2.6. Post-Hoc Analyses on Clinical Variables

Several post-hoc analyses were performed to explore the potential influence of disease chronicity and medications. First, the temporal correlation coefficients of whole brain or any network with significant between-group differences were correlated with the MDD patients' illness duration. Second, the temporal correlation coefficients with significant between-group differences were compared between the drug-naïve and medicated MDD patients using the ANCOVA covarying for age, sex, and education. Third, the temporal correlation coefficients with significant between-group differences were correlated with the MDD patients' daily doses of antidepressant as assessed by fluoxetine equivalents [45]. Significance was set at $p < 0.05$.

2.7. Validation Analyses

A number of supplementary analyses were further performed to validate the results. First, all correlation analyses on the temporal correlation coefficients were repeated with patients' daily doses of antidepressant (fluoxetine equivalents) as an additional covariate (using the partial Spearman's correlations). Second, the relationships between temporal correlation coefficients and HAMD item 3 scores were investigated using an ordinal logistic regression model [46], to see whether the observed significant relationships would change in different statistical models.

3. Results

3.1. Demographic Characteristics and Head Motion

As shown in Table 1, there were no significant between-group differences in age and sex (all $p > 0.05$). However, the groups of MDD showed a significantly lower education level ($t = -3.571$, $p = 0.001$). There was no significant between-group difference in head motion as measured by mean FD ($t = 1.288$, $p = 0.202$).

Table 1. Demographic, clinical, and head motion characteristics of the groups. SD, standard deviation; MDD, major depressive disorder; HCs, healthy controls; HAMD, Hamilton Rating Scale for Depression; FD, framewise-displacement.

	MDD (n = 52) (Mean ± SD)	HCs (n = 21) (Mean ± SD)	Group Comparisons
Age (years)	30.615 ± 9.306	27.000 ± 5.908	$t = 1.982$, $p = 0.052$
Sex (male/female)	28/24	10/11	$\chi^2 = 0.232$, $p = 0.796$
Education (years)	12.115 ± 3.191	14.952 ± 2.747	$t = -3.571$, $p = 0.001$
17-item HAMD scores	20.789 ± 6.366	/	/
HAMD item 3 scores	1.769 ± 1.246	/	/
Illness duration (months)	42.919 ± 62.291	/	/
Drug-naïve/medicated	9/43	/	/
Fluoxetine equivalents (mg/d)	25.360 ± 20.024		
Mean FD	0.086 ± 0.038	0.074 ± 0.030	$t = 1.288$, $p = 0.202$

3.2. MDD-Related Alterations

As shown in Figure 2, the MDD patients showed a significantly decreased temporal correlation coefficient of the whole brain than HCs ($F = 8.014$, $p = 0.006$); moreover, the MDD patients showed a significantly decreased temporal correlation coefficient of the DMN ($F = 7.526$, FDR-corrected $p = 0.035$) and subcortical network ($F = 9.885$, FDR-corrected $p = 0.022$). The components of the DMN and subcortical network, which showed significant between-group differences, were also presented in Figure 3. No significant between-group differences were found in other networks (all $p > 0.05$).

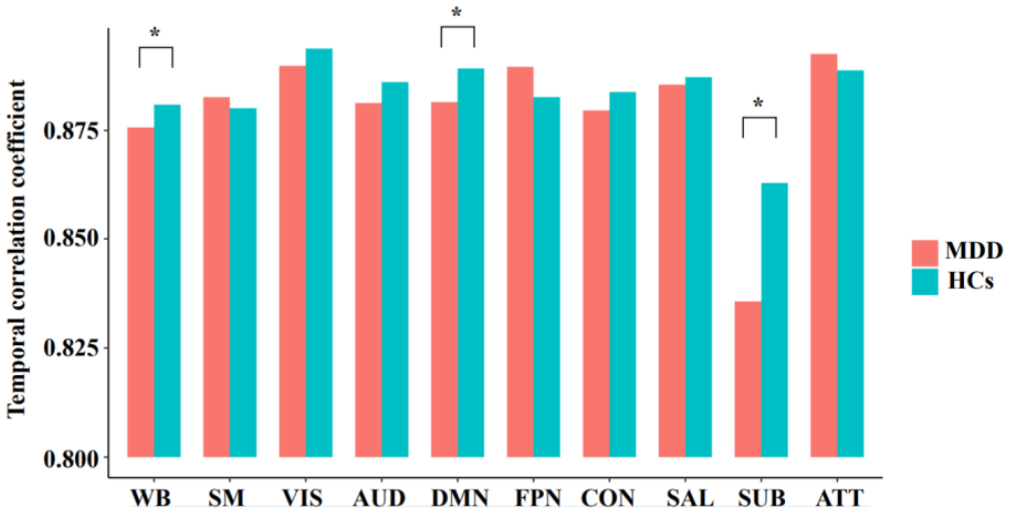

Figure 2. The mean temporal correlation coefficients of the whole brain and each network in the groups of major depressive disorder (MDD) and healthy controls (HCs), after adjusting for age, sex, and education. WB, whole brain; SM, sensorimotor network; VIS, visual network; AUD, auditory network; DMN, default mode network; FPN, frontoparietal network; CON, cingulo-opercular network; SAL, salience network; SUB, subcortical network; ATT, attention network; * significant difference with corrected $p < 0.05$.

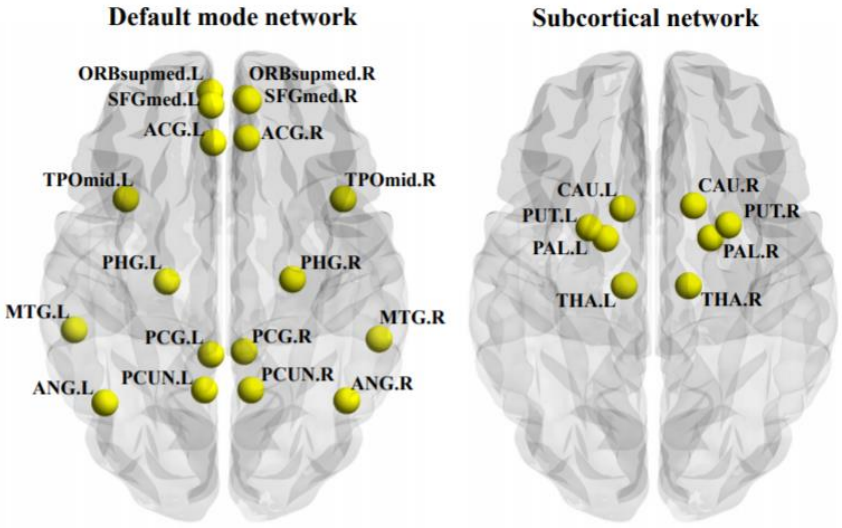

Figure 3. The components of the default mode network and subcortical network, of which the temporal correlation coefficients were significantly decreased in the patients with major depressive disorder. ACG, anterior cingulate cortex; ANG, angular gyrus; CAU, caudate; L, left hemisphere; MTG, middle temporal gyrus; ORBsupmed, medial orbitofrontal cortex; PAL, pallidum; PCUN, precuneus; PHG, parahippocampal gyrus; PUT, putamen; R, right hemisphere; SFGmed, medial superior frontal cortex; SPG, superior parietal gyrus; THA, thalamus; TPOmid, middle temporal pole.

3.3. Correlations

In MDD patients, the scores of HAMD item 3 were found to significantly negatively correlated with the temporal correlation coefficient of the DMN (Spearman's rho = −0.371, FDR-corrected $p = 0.021$, Figure 4) but not with the temporal correlation coefficient of whole brain or any other network (all $p > 0.05$). No significant correlations were found between the total scores of HAMD and the temporal correlation coefficient of whole brain or any network, either (all $p > 0.05$).

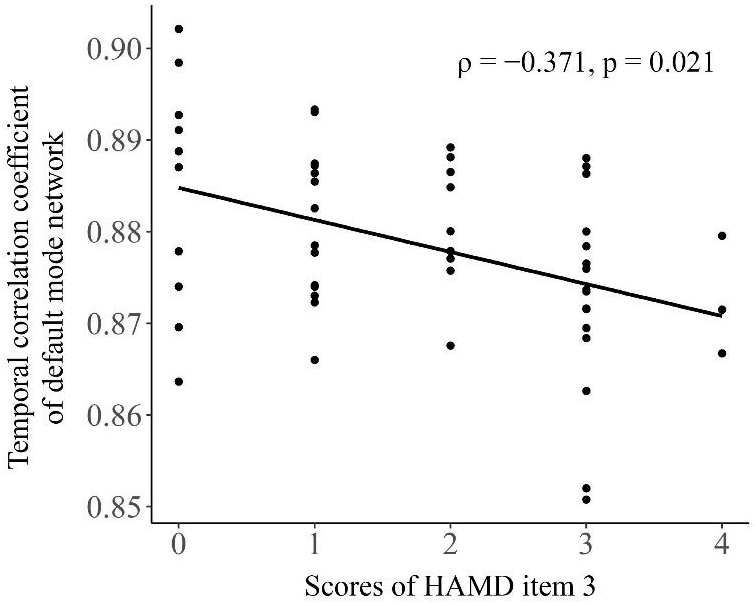

Figure 4. The relationship between the temporal correlation coefficient of default mode network and the scores of HAMD item 3 in the patients with major depressive disorder. The Spearman's correlation coefficient (ρ) and FDR-corrected *p* value were presented on the figure.

3.4. Post-Hoc Analyses on Clinical Variables

No significant correlations were found between the MDD patients' illness duration and temporal correlation coefficients of the whole brain or any network (all $p > 0.05$). No significant differences were found in temporal correlation coefficients between the drug-naïve and medicated MDD patients (all $p > 0.05$). Additionally, no significant correlations were found between the temporal correlation coefficients and MDD patients' daily doses of antidepressant assessed by fluoxetine equivalents (all $p > 0.05$).

3.5. Validation Analyses

The negative correlation between the temporal correlation coefficient of DMN and scores of HAMD item 3 in MDD patients remained significant when including the patients' daily doses of antidepressant as an additional covariate (Spearman's rho = −0.370, $p = 0.008$). Therefore, such a relationship is unlikely to be mainly driven by effects of medication treatment. Furthermore, when using an ordinal logistic regression model, it was still found that the temporal correlation coefficient of DMN is significantly negatively associated with the scores of HAMD item 3 ($z = -2.494$, $p = 0.013$).

4. Discussion

The present study, to the best of our knowledge, investigated the alterations in temporal stability of brain dFC and their associations with suicidality in MDD using the dynamic network model and temporal correlation coefficient for the first time. Our major findings were: (1) compared with HCs, the MDD patients exhibited a significantly decreased temporal correlation coefficient of the whole brain, and significantly decreased temporal correlation coefficients of the DMN and subcortical network; (2) the temporal correlation coefficient of the DMN was significantly negatively related with the suicidality in MDD patients. Our findings may expand our understanding of the neurophysiologic mechanisms of the suicidality in MDD.

The decreased temporal correlation coefficient indicates a lower tendency for the brain dFC patterns to be maintained over time or in other words, a decreased temporal stability (increased temporal variability) of dFC [12,21]. Compared with HCs, the MDD patients showed a significantly decreased temporal correlation coefficient of the whole brain, suggesting an excessive fluctuation of FC at the global level. Furthermore, significant local alterations were found in the DMN and subcortical network, which may indicate the prominent excessive fluctuations of these two brain systems (Figure 2). The results were compatible with the prior work which reported an increased variability of FC within the DMN [12,13] and subcortical structures [14] in MDD.

We found that the temporal correlation coefficient of the DMN were significantly negatively related to the scores of the HAMD suicidality item in MDD patients (Figure 4). The result suggests that the excessive fluctuations of dFC within the DMN may underly the psychopathology of suicidality in MDD. The DMN is a brain network which are more active during rest but suppressed during cognitive activities including several distributed nodes such as the precuneus, anterior cingulate cortex, posterior cingulate cortex, and medial prefrontal cortex (Figure 3) [47–49]. In MDD patients, static FC patterns within the DMN are often found to be changed [31,49,50] and such changes have been reported to be related to their suicidal thoughts or attempts [3,51,52] in traditional static fMRI studies. The associations between the changes in dFC within the DMN and suicidality in MDD, however, are relatively limited. The DMN were suggested to mediate one's self-referential and internally directed processing [49,53]. In healthy subjects, the increased variability of dFC within the DMN has been proved to be associated with increased frequencies of spontaneous, internally oriented thoughts such as mind-wandering during the resting state [54,55]. In MDD patients, the increased variability of dFC within the DMN has been also reported to be related with their frequencies of rumination [11,13], a characteristic form of spontaneous, negative, and internally oriented thought defined as "repetitively and passively focusing on symptoms of distress" [56,57]. Therefore, we assume that the

excessive variability of the DMN connections may be an indicative of repetitive abnormal activations of the DMN, which lead to excessive negative, internally focused thoughts such as rumination in MDD patients. Such alterations may make the MDD patients more focused on their negative life events and more vulnerable to thinking about suicide, which lead to higher suicidality [58,59]. Our findings, therefore, may extend the finding of the association between abnormal DMN connectivity and suicidality in MDD [3,51,52] into the domain of dynamic brain FC.

In the MDD patients, the decreased temporal stability (increased variability) of dFC as indicated by a significantly decreased temporal correlation coefficient was also observed within the subcortical network including the thalamus, putamen, pallidum and caudate (Figure 4). This result is in line with a recent study which reported an increased variability of dFC in the pallidum in MDD and suggested that it may imply the impaired reward processing [14]. The temporal correlation coefficient of the subcortical network, however, was not significantly correlated with the suicidality in MDD patients. No significant correlation was found between the temporal correlation coefficient of the whole brain and suicidality in MDD, either. Therefore, the excessive variability of dFC within the DMN may be a unique biomarker of the suicidality in MDD.

Our study has several limitations. First, the education level was not matched between the groups of MDD and HCs. To solve this problem, we used the education level as a covariant in the group comparisons to exclude its effect as a potential confounding factor. Second, the suicidality was measured by only the item 3 of HAMD. In the future, a more detailed scale for suicide such as the Columbia Suicide Severity Rating Scale [26] is necessary for more detailed analysis, for example, to distinguish the possible differences be-tween the patients with active and passive suicidal ideation [60]. Third, the sample size in the present study is relatively small and larger samples are needed to confirm our findings. Fourth, the HAMD was not assessed in HCs, and we are unable to confirm whether similar effects would exist in HCs. Fifth, because of the nature of a cross-sectional design, we are unable to establish the causality relationship between the suicidality and brain network stability in MDD patients. Lastly, while a decreased temporal stability of DMN dFC pattern was found in MDD in the present study, it should be noted that reports of an increased stability of DMN dFC in MDD patients also exist [61,62]. It is possible that subtypes of MDD with distinct DMN dFC profiles (hypo- and hyper-stability) could exist [63], which can be investigated in future studies.

5. Conclusions

To conclude, using a dynamic brain network model and temporal correlation coefficient, the present study identified a significantly decreased temporal stability (increased variability) of brain dFC at the global level, as well as within the DMN and subcortical network in MDD patients. Moreover, we found that decreased temporal stability of dFC within the DMN was significantly related to higher suicidality in the MDD patients. These findings may have important implications for better understanding and preventing suicide in MDD.

Author Contributions: Conceptualization, X.O., Y.L. and X.H.; methodology, X.O. and Y.L.; software, Y.L.; validation, X.H.; formal analysis, X.O., Y.L. and X.H.; investigation, X.O., Y.L., Z.W., D.L. and X.H.; resources, X.O., Y.L. and X.H.; data curation, Y.L.; writing—original draft preparation, X.O. and Y.L.; writing—review and editing, Z.L. and X.H.; visualization, Y.L.; supervision, Z.L. and X.H.; project administration, Z.L. and X.H.; funding acquisition, Y.L., Z.L. and X.H. All authors have read and agreed to the published version of the manuscript.

Funding: This research was funded by the Natural Science Foundation of Hunan Province, China (grant numbers 2021JJ40851 and 2021JJ40835), the Changsha Municipal Natural Science Foundation (kq2014238), and the National Natural Science Foundation of China (grant number 82071506).

Institutional Review Board Statement: The study was conducted in accordance with the Declaration of Helsinki, and approved by the ethics committee of the Second Xiangya Hospital, Central South University (IRB number 2016S024).

Informed Consent Statement: Informed consent was obtained from all subjects involved in the study.

Data Availability Statement: The data presented in this study are available on request from the corresponding author.

Acknowledgments: The authors would like to thank Hengyi Cao from Feinstein Institute for Medical Research, New York, USA, who gave some suggestions during the preparation of this manuscript.

Conflicts of Interest: The authors declare no conflict of interest.

Appendix A

Table A1. List of the 90 regions of interest used in the present study and their network affiliations based on prior research. Odd and even numbers represent left and right hemispheres, respectively.

Index	Corresponding Brain Region	Network Affiliation
(1,2)	Precentral gyrus	Sensorimotor
(3,4)	Superior frontal gyrus, dorsolateral	Frontoparietal
(5,6)	Superior frontal gyrus, orbital part	Frontoparietal
(7,8)	Middle frontal gyrus	Salience/frontoparietal/attention
(9,10)	Middle frontal gyrus, orbital part	Frontoparietal
(11,12)	Inferior frontal gyrus, opercular part	Cingulo-opercular
(13,14)	Inferior frontal gyrus, triangular part	Salience/frontoparietal/attention
(15,16)	Inferior frontal gyrus, orbital part	None
(17,18)	Rolandic operculum	Auditory/cingulo-opercular
(19,20)	Supplementary motor area	Sensorimotor
(21,22)	Olfactory cortex	None
(23,24)	Superior frontal gyrus, medial	Default-mode
(25,26)	Superior frontal gyrus, medial orbital	Default-mode
(27,28)	Gyrus rectus	None
(29,30)	Insula	Salience/cingulo-opercular
(31,32)	Anterior cingulate and paracingulate gyri	Default-mode/salience
(33,34)	Median cingulate and paracingulate gyri	Salience/cingulo-opercular
(35,36)	Posterior cingulate gyrus	Default-mode
(37,38)	Hippocampus	None
(39,40)	Parahippocampal gyrus	Default-mode
(41,42)	Amygdala	None
(43,44)	Calcarine fissure and surrounding cortex	Visual
(45,46)	Cuneus	Visual
(47,48)	Lingual gyrus	Visual
(49,50)	Superior occipital gyrus	Visual
(51,52)	Middle occipital gyrus	Visual
(53,54)	Inferior occipital gyrus	Visual
(55,56)	Fusiform gyrus	Visual
(57,58)	Postcentral gyrus	Sensorimotor
(59,60)	Superior parietal gyrus	Salience/attention
(61,62)	Inferior parietal, but supramarginal and angular gyri	Frontoparietal/attention
(63,64)	Supramarginal gyrus	Auditory/cingulo-opercular
(65,66)	Angular gyrus	Default-mode
(67,68)	Precuneus	Default-mode
(69,70)	Paracentral lobule	Sensorimotor
(71,72)	Caudate nucleus	Subcortical
(73,74)	Lenticular nucleus, putamen	Subcortical
(75,76)	Lenticular nucleus, pallidum	Subcortical
(77,78)	Thalamus	Thalamus
(79,80)	Heschl gyrus	Auditory
(81,82)	Superior temporal gyrus	Auditory/attention
(83,84)	Temporal pole: superior temporal gyrus	Cingulo-opercular
(85,86)	Middle temporal gyrus	Default-mode
(87,88)	Temporal pole: middle temporal gyrus	Default-mode
(89,90)	Inferior temporal gyrus	None

References

1. Kassebaum, N.J.; Arora, M.; Barber, R.M.; Brown, J.; Carter, A.; Casey, D.C.; Charlson, F.J.; Coates, M.M.; Coggeshall, M.; Cornaby, L.; et al. Global, Regional, and National Disability-Adjusted Life-Years (DALYs) for 315 Diseases and Injuries and Healthy Life Expectancy (HALE), 1990–2015: A Systematic Analysis for the Global Burden of Disease Study 2015. *Lancet* **2016**, *388*, 1603–1658. [CrossRef]
2. Iancu, S.C.; Wong, Y.M.; Rhebergen, D.; van Balkom, A.J.L.M.; Batelaan, N.M. Long-Term Disability in Major Depressive Disorder: A 6-Year Follow-up Study. *Psychol. Med.* **2020**, *50*, 1644–1652. [CrossRef] [PubMed]
3. Schreiner, M.W.; Klimes-Dougan, B.; Cullen, K.R. Neural Correlates of Suicidality in Adolescents with Major Depression: Resting-State Functional Connectivity of the Precuneus and Posterior Cingulate Cortex. *Suicide Life Threat. Behav.* **2019**, *49*, 899–913. [CrossRef] [PubMed]

4. Wei, S.; Chang, M.; Zhang, R.; Jiang, X.; Wang, F.; Tang, Y. Amygdala Functional Connectivity in Female Patients with Major Depressive Disorder with and without Suicidal Ideation. *Ann. Gen. Psychiatry* **2018**, *17*, 37. [CrossRef] [PubMed]
5. Du, L.; Zeng, J.; Liu, H.; Tang, D.; Meng, H.; Li, Y.; Fu, Y. Fronto-Limbic Disconnection in Depressed Patients with Suicidal Ideation: A Resting-State Functional Connectivity Study. *J. Affect. Disord.* **2017**, *215*, 213–217. [CrossRef]
6. Hutchison, R.M.; Womelsdorf, T.; Gati, J.S.; Everling, S.; Menon, R.S. Resting-State Networks Show Dynamic Functional Connectivity in Awake Humans and Anesthetized Macaques. *Hum. Brain Mapp.* **2013**, *34*, 2154–2177. [CrossRef]
7. Hutchison, R.M.; Womelsdorf, T.; Allen, E.A.; Bandettini, P.A.; Calhoun, V.D.; Corbetta, M.; della Penna, S.; Duyn, J.H.; Glover, G.H.; Gonzalez-Castillo, J.; et al. Dynamic Functional Connectivity: Promise, Issues, and Interpretations. *Neuroimage* **2013**, *80*, 360–378. [CrossRef]
8. Preti, M.G.; Bolton, T.A.; van de Ville, D. The Dynamic Functional Connectome: State-of-the-Art and Perspectives. *Neuroimage* **2017**, *160*, 41–54. [CrossRef]
9. Huang, D.; Liu, Z.; Cao, H.; Yang, J.; Wu, Z.; Long, Y. Childhood Trauma Is Linked to Decreased Temporal Stability of Functional Brain Networks in Young Adults. *J. Affect. Disord.* **2021**, *290*, 23–30. [CrossRef]
10. Lin, Z.; Long, Y.; Wu, Z.; Xiang, Z.; Ju, Y.; Liu, Z. Associations between Brain Abnormalities and Common Genetic Variants for Schizophrenia: A Narrative Review of Structural and Functional Neuroimaging Findings. *Ann. Palliat. Med.* **2021**, *10*, 10031–10052. [CrossRef]
11. Kaiser, R.H.; Whitfield-Gabrieli, S.; Dillon, D.G.; Goer, F.; Beltzer, M.; Minkel, J.; Smoski, M.; Dichter, G.; Pizzagalli, D.A. Dynamic Resting-State Functional Connectivity in Major Depression. *Neuropsychopharmacology* **2016**, *41*, 1822–1830. [CrossRef] [PubMed]
12. Long, Y.; Cao, H.; Yan, C.; Chen, X.; Li, L.; Castellanos, F.X.; Bai, T.; Bo, Q.; Chen, G.; Chen, N.; et al. Altered Resting-State Dynamic Functional Brain Networks in Major Depressive Disorder: Findings from the REST-Meta-MDD Consortium. *Neuroimage Clin.* **2020**, *26*, 102163. [CrossRef] [PubMed]
13. Wise, T.; Marwood, L.; Perkins, A.M.; Herane-Vives, A.; Joules, R.; Lythgoe, D.J.; Luh, W.M.; Williams, S.C.R.; Young, A.H.; Cleare, A.J.; et al. Instability of Default Mode Network Connectivity in Major Depression: A Two-Sample Confirmation Study. *Transl. Psychiatry* **2017**, *7*, e1105. [CrossRef]
14. Hou, Z.; Kong, Y.; He, X.; Yin, Y.; Zhang, Y.; Yuan, Y. Increased Temporal Variability of Striatum Region Facilitating the Early Antidepressant Response in Patients with Major Depressive Disorder. *Prog. Neuropsychopharmacol. Biol. Psychiatry* **2018**, *85*, 39–45. [CrossRef] [PubMed]
15. Liao, W.; Li, J.; Duan, X.; Cui, Q.; Chen, H.; Chen, H. Static and Dynamic Connectomics Differentiate between Depressed Patients with and without Suicidal Ideation. *Hum. Brain Mapp.* **2018**, *39*, 4105–4118. [CrossRef] [PubMed]
16. Yang, J.; Liu, Z.; Tao, H.; Cheng, Y.; Fan, Z.; Sun, F.; Ouyang, X.; Yang, J. Aberrant Brain Dynamics in Major Depressive Disorder with Suicidal Ideation. *J. Affect. Disord.* **2022**, *314*, 263–270. [CrossRef]
17. Li, J.; Duan, X.; Cui, Q.; Chen, H.; Liao, W. More than Just Statics: Temporal Dynamics of Intrinsic Brain Activity Predicts the Suicidal Ideation in Depressed Patients. *Psychol. Med.* **2019**, *49*, 852–860. [CrossRef]
18. Qiao, D.; Zhang, A.; Sun, N.; Yang, C.; Li, J.; Zhao, T.; Wang, Y.; Xu, Y.; Wen, Y.; Zhang, K.; et al. Altered Static and Dynamic Functional Connectivity of Habenula Associated With Suicidal Ideation in First-Episode, Drug-Naïve Patients With Major Depressive Disorder. *Front. Psychiatry* **2020**, *11*, 608197. [CrossRef]
19. Zuberer, A.; Kucyi, A.; Yamashita, A.; Wu, C.M.; Walter, M.; Valera, E.M.; Esterman, M. Integration and Segregation across Large-Scale Intrinsic Brain Networks as a Marker of Sustained Attention and Task-Unrelated Thought. *Neuroimage* **2021**, *229*, 117610. [CrossRef]
20. Long, Y.; Liu, Z.; Chan, C.K.Y.; Wu, G.; Xue, Z.; Pan, Y.; Chen, X.; Huang, X.; Li, D.; Pu, W. Altered Temporal Variability of Local and Large-Scale Resting-State Brain Functional Connectivity Patterns in Schizophrenia and Bipolar Disorder. *Front. Psychiatry* **2020**, *11*, 422. [CrossRef]
21. Sizemore, A.E.; Bassett, D.S. Dynamic Graph Metrics: Tutorial, Toolbox, and Tale. *Neuroimage* **2018**, *180*, 417–427. [CrossRef] [PubMed]
22. Long, Y.; Yan, C.; Wu, Z.; Huang, X.; Cao, H.; Liu, Z.; Palaniyappan, L. Evaluating Test-Retest Reliability and Sex/Age-Related Effects on Temporal Clustering Coefficient of Dynamic Functional Brain Networks. *bioRxiv* **2021**. [CrossRef]
23. Yi, G.; Wang, L.; Chu, C.; Liu, C.; Zhu, X.; Shen, X.; Li, Z.; Wang, F.; Yang, M.; Wang, J. Analysis of Complexity and Dynamic Functional Connectivity Based on Resting-State EEG in Early Parkinson's Disease Patients with Mild Cognitive Impairment. *Cogn. Neurodyn.* **2022**, *16*, 309–323. [CrossRef] [PubMed]
24. Power, J.D.; Cohen, A.L.; Nelson, S.M.; Wig, G.S.; Barnes, K.A.; Church, J.A.; Vogel, A.C.; Laumann, T.O.; Miezin, F.M.; Schlaggar, B.L.; et al. Functional Network Organization of the Human Brain. *Neuron* **2011**, *72*, 665–678. [CrossRef]
25. Cao, H.; Chung, Y.; McEwen, S.C.; Bearden, C.E.; Addington, J.; Goodyear, B.; Cadenhead, K.S.; Mirzakhanian, H.; Cornblatt, B.A.; Carrión, R.; et al. Progressive Reconfiguration of Resting-State Brain Networks as Psychosis Develops: Preliminary Results from the North American Prodrome Longitudinal Study (NAPLS) Consortium. *Schizophr. Res.* **2019**, *226*, 30–37. [CrossRef]
26. Long, Y.; Ouyang, X.; Liu, Z.; Chen, X.; Hu, X.; Lee, E.; Chen, E.Y.H.; Pu, W.; Shan, B.; Rohrbaugh, R.M. Associations among Suicidal Ideation, White Matter Integrity and Cognitive Deficit in First-Episode Schizophrenia. *Front. Psychiatry* **2018**, *9*, 391. [CrossRef]
27. Pu, S.; Nakagome, K.; Yamada, T.; Yokoyama, K.; Matsumura, H.; Yamada, S.; Sugie, T.; Miura, A.; Mitani, H.; Iwata, M.; et al. Suicidal Ideation Is Associated with Reduced Prefrontal Activation during a Verbal Fluency Task in Patients with Major Depressive Disorder. *J. Affect. Disord.* **2015**, *181*, 9–17. [CrossRef]

28. Park, Y.M.; Lee, B.H.; Lee, S.H. The Association between Serum Lipid Levels, Suicide Ideation, and Central Serotonergic Activity in Patients with Major Depressive Disorder. *J. Affect. Disord.* **2014**, *159*, 62–65. [CrossRef]
29. Yan, C.G.; Wang, X.-D.; Zuo, X.N.; Zang, Y.F. DPABI: Data Processing & Analysis for (Resting-State) Brain Imaging. *Neuroinformatics* **2016**, *14*, 339–351. [CrossRef]
30. Chao-Gan, Y.; Yu-Feng, Z. DPARSF: A MATLAB Toolbox for "Pipeline" Data Analysis of Resting-State FMRI. *Front. Syst. Neurosci.* **2010**, *4*, 13. [CrossRef]
31. Yan, C.G.; Chen, X.; Li, L.; Castellanos, F.X.; Bai, T.J.; Bo, Q.J.; Cao, J.; Chen, G.M.; Chen, N.X.; Chen, W.; et al. Reduced Default Mode Network Functional Connectivity in Patients with Recurrent Major Depressive Disorder. *Proc. Natl. Acad. Sci. USA* **2019**, *116*, 9078–9083. [CrossRef] [PubMed]
32. Huang, X.; Wu, Z.; Liu, Z.; Liu, D.; Huang, D.; Long, Y. Acute Effect of Betel Quid Chewing on Brain Network Dynamics: A Resting-State Functional Magnetic Resonance Imaging Study. *Front. Psychiatry* **2021**, *12*, 701420. [CrossRef] [PubMed]
33. Jenkinson, M.; Bannister, P.; Brady, M.; Smith, S. Improved Optimization for the Robust and Accurate Linear Registration and Motion Correction of Brain Images. *Neuroimage* **2002**, *17*, 825–841. [CrossRef] [PubMed]
34. Tzourio-Mazoyer, N.; Landeau, B.; Papathanassiou, D.; Crivello, F.; Etard, O.; Delcroix, N.; Mazoyer, B.; Joliot, M. Automated Anatomical Labeling of Activations in SPM Using a Macroscopic Anatomical Parcellation of the MNI MRI Single-Subject Brain. *Neuroimage* **2002**, *15*, 273–289. [CrossRef]
35. Cao, H.; Bertolino, A.; Walter, H.; Schneider, M.; Schafer, A.; Taurisano, P.; Blasi, G.; Haddad, L.; Grimm, O.; Otto, K.; et al. Altered Functional Subnetwork during Emotional Face Processing a Potential Intermediate Phenotype for Schizophrenia. *JAMA Psychiatry* **2016**, *73*, 598–605. [CrossRef]
36. Cao, H.; Plichta, M.M.; Schäfer, A.; Haddad, L.; Grimm, O.; Schneider, M.; Esslinger, C.; Kirsch, P.; Meyer-Lindenberg, A.; Tost, H. Test-Retest Reliability of FMRI-Based Graph Theoretical Properties during Working Memory, Emotion Processing, and Resting State. *Neuroimage* **2014**, *84*, 888–900. [CrossRef]
37. Zhang, C.; Baum, S.A.; Adduru, V.R.; Biswal, B.B.; Michael, A.M. Test-Retest Reliability of Dynamic Functional Connectivity in Resting State FMRI. *Neuroimage* **2018**, *183*, 907–918. [CrossRef]
38. Sun, Y.; Collinson, S.L.; Suckling, J.; Sim, K. Dynamic Reorganization of Functional Connectivity Reveals Abnormal Temporal Efficiency in Schizophrenia. *Schizophr. Bull.* **2019**, *45*, 659–669. [CrossRef] [PubMed]
39. Tang, S.; Wu, Z.; Cao, H.; Chen, X.; Wu, G.; Tan, W.; Liu, D.; Yang, J.; Long, Y.; Liu, Z. Age-Related Decrease in Default-Mode Network Functional Connectivity Is Accelerated in Patients With Major Depressive Disorder. *Front. Aging Neurosci.* **2022**, *13*, 809853. [CrossRef]
40. Liu, D.; Tang, S.; Wu, Z.; Yang, J.; Liu, Z.; Wu, G.; Sariah, A.; Ouyang, X.; Long, Y. Changes in Brain Network Properties in Major Depressive Disorder Following Electroconvulsive Therapy: A Combined Static and Dynamic Functional Magnetic Resonance Imaging Study. *Ann. Palliat. Med.* **2022**, *11*, 1969–1980. [CrossRef]
41. Tang, J.; Scellato, S.; Musolesi, M.; Mascolo, C.; Latora, V. Small-World Behavior in Time-Varying Graphs. *Phys. Rev. E Cover. Stat. Nonlinear Soft Matter Phys.* **2010**, *81*, 055101. [CrossRef] [PubMed]
42. Long, Y.; Chen, C.; Deng, M.; Huang, X.; Tan, W.; Zhang, L.; Fan, Z.; Liu, Z. Psychological Resilience Negatively Correlates with Resting-State Brain Network Flexibility in Young Healthy Adults: A Dynamic Functional Magnetic Resonance Imaging Study. *Ann. Transl. Med.* **2019**, *7*, 809. [CrossRef] [PubMed]
43. Rubinov, M.; Sporns, O. Complex Network Measures of Brain Connectivity: Uses and Interpretations. *Neuroimage* **2010**, *52*, 1059–1069. [CrossRef] [PubMed]
44. Xia, M.; Wang, J.; He, Y. BrainNet Viewer: A Network Visualization Tool for Human Brain Connectomics. *PLoS ONE* **2013**, *8*, e68910. [CrossRef] [PubMed]
45. Hayasaka, Y.; Purgato, M.; Magni, L.R.; Ogawa, Y.; Takeshima, N.; Cipriani, A.; Barbui, C.; Leucht, S.; Furukawa, T.A. Dose Equivalents of Antidepressants: Evidence-Based Recommendations from Randomized Controlled Trials. *J. Affect. Disord.* **2015**, *180*, 179–184. [CrossRef] [PubMed]
46. Jaspers-Fayer, F.; Lin, S.Y.; Chan, E.; Ellwyn, R.; Lim, R.; Best, J.; Belschner, L.; Lang, D.; Heran, M.K.M.; Woodward, T.S.; et al. Neural Correlates of Symptom Provocation in Pediatric Obsessive-Compulsive Disorder. *Neuroimage Clin.* **2019**, *24*, 102034. [CrossRef]
47. Davey, C.G.; Pujol, J.; Harrison, B.J. Mapping the Self in the Brain's Default Mode Network. *Neuroimage* **2016**, *132*, 390–397. [CrossRef]
48. Raichle, M.E. The Brain's Default Mode Network. *Annu. Rev. Neurosci.* **2015**, *38*, 433–447. [CrossRef]
49. Whitfield-Gabrieli, S.; Ford, J.M. Default Mode Network Activity and Connectivity in Psychopathology. *Annu. Rev. Clin. Psychol.* **2012**, *8*, 49–76. [CrossRef]
50. Zhu, X.; Wang, X.; Xiao, J.; Liao, J.; Zhong, M.; Wang, W.; Yao, S. Evidence of a Dissociation Pattern in Resting-State Default Mode Network Connectivity in First-Episode, Treatment-Naive Major Depression Patients. *Biol. Psychiatry* **2012**, *71*, 611–617. [CrossRef]
51. Fan, T.; Wu, X.; Yao, L.; Dong, J. Abnormal Baseline Brain Activity in Suicidal and Non-Suicidal Patients with Major Depressive Disorder. *Neurosci. Lett.* **2013**, *534*, 35–40. [CrossRef] [PubMed]
52. Zhang, S.; Chen, J.; Kuang, L.; Cao, J.; Zhang, H.; Ai, M.; Wang, W.; Zhang, S.; Wang, S.; Liu, S.; et al. Association between Abnormal Default Mode Network Activity and Suicidality in Depressed Adolescents. *BMC Psychiatry* **2016**, *16*, 337. [CrossRef] [PubMed]
53. Zhou, L.; Pu, W.; Wang, J.; Liu, H.; Wu, G.; Liu, C.; Mwansisya, T.E.; Tao, H.; Chen, X.; Huang, X.; et al. Inefficient DMN Suppression in Schizophrenia Patients with Impaired Cognitive Function but Not Patients with Preserved Cognitive Function. *Sci. Rep.* **2016**, *6*, 21657. [CrossRef] [PubMed]

54. Kucyi, A.; Davis, K.D. Dynamic Functional Connectivity of the Default Mode Network Tracks Daydreaming. *Neuroimage* **2014**, *100*, 471–480. [CrossRef] [PubMed]
55. Zabelina, D.L.; Andrews-Hanna, J.R. Dynamic Network Interactions Supporting Internally-Oriented Cognition. *Curr. Opin. Neurobiol.* **2016**, *40*, 86–93. [CrossRef]
56. Nolen-Hoeksema, S.; Wisco, B.E.; Lyubomirsky, S. Rethinking Rumination. *Perspect. Psychol. Sci.* **2008**, *3*, 400–424. [CrossRef]
57. Kucyi, A.; Tambini, A.; Sadaghiani, S.; Keilholz, S.; Cohen, J.R. Spontaneous Cognitive Processes and the Behavioral Validation of Time-Varying Brain Connectivity. *Netw. Neurosci.* **2018**, *2*, 397–417. [CrossRef]
58. Surrence, K.; Miranda, R.; Marroquín, B.M.; Chan, S. Brooding and Reflective Rumination among Suicide Attempters: Cognitive Vulnerability to Suicidal Ideation. *Behav. Res. Ther.* **2009**, *47*, 803–808. [CrossRef]
59. Chan, S.; Miranda, R.; Surrence, K. Subtypes of Rumination in the Relationship between Negative Life Events and Suicidal Ideation. *Arch. Suicide Res.* **2009**, *13*, 123–135. [CrossRef]
60. Szanto, K.; Reynolds, C.F.; Frank, E.; Stack, J.; Fasiczka, A.L.; Miller, M.; Mulsant, B.H.; Mazumdar, S.; Kupfer, D.J. Suicide in Elderly Depressed Patients: Is Active vs. Passive Suicidal Ideation a Clinically Valid Distinction? *Am. J. Geriatr. Psychiatry* **1996**, *4*, 197–207. [CrossRef]
61. Piguet, C.; Karahanoğlu, F.I.; Saccaro, L.F.; van de Ville, D.; Vuilleumier, P. Mood Disorders Disrupt the Functional Dynamics, Not Spatial Organization of Brain Resting State Networks. *Neuroimage Clin.* **2021**, *32*, 102833. [CrossRef] [PubMed]
62. Demirtaş, M.; Tornador, C.; Falcón, C.; López-Solà, M.; Hernández-Ribas, R.; Pujol, J.; Menchón, J.M.; Ritter, P.; Cardoner, N.; Soriano-Mas, C.; et al. Dynamic Functional Connectivity Reveals Altered Variability in Functional Connectivity among Patients with Major Depressive Disorder. *Hum. Brain Mapp.* **2016**, *37*, 2918–2930. [CrossRef] [PubMed]
63. Liang, S.; Deng, W.; Li, X.; Greenshaw, A.J.; Wang, Q.; Li, M.; Ma, X.; Bai, T.J.; Bo, Q.J.; Cao, J.; et al. Biotypes of Major Depressive Disorder: Neuroimaging Evidence from Resting-State Default Mode Network Patterns. *Neuroimage Clin.* **2020**, *28*, 102514. [CrossRef] [PubMed]